Proceedings of the 20th International Conference on Soil Mechanics and Geotechnical Engineering– Rahman and Jaksa (Eds)

Simulation of pile penetration in sand employing Lagrangian and CEL based FE approach: a comparative study

Mousumi Mukherjee & Bhupendra Chand
School of Engineering, Indian Institute of Technology Mandi, India, mousumi.ju06@gmail.com

ABSTRACT: Pile penetration process is usually associated with excessive deformation which makes its numerical simulation very challenging. Updated Lagrangian formulation can simulate such boundary value problems involving large deformation in conjunction with application of proper analysis control. On the contrary, Coupled Eulerian-Lagrangian (CEL) framework, employed recently to model many complex geotechnical engineering problems, has advantages of both Eulerian and Lagrangian formulation. In the present study, pile penetration process has been simulated in ABAQUS software employing both updated Lagrangian and CEL formulation in order to compare their effectiveness in replicating such large deformation process. Mohr coulomb type soil constitutive model and penalty stiffness-based contact modelling has been adopted for the pile-soil interaction. The evolution of stress-strain components at pile-soil interafce and along the horizontal paths, toe and shaft resistance during the complete penetration process has been compared for these two frameworks with due consideration to the influence of mesh discretization. The influence of penetration rate and soil-pile interface friction has also been examined on the predicted response. Further, the phenomena associated with driven piles, i.e. friction fatigue during the driving process and generation of residual stress in the post-driving period has also been explored.

KEYWORDS: Pile penetration, updated Lagrangian, CEL, friction fatigue, residual stress.

1 INTRODUCTION.

Pile foundations are typically used to transfer load through the weak soil to the hard strata and their installation process involves large deformations. The high expenses associated with the field studies often restricts the numbers of pile testing which may lead to estimation of inappropriate pile strength. In this context, numerical simulation could be a better choice to explore the performance of the piles under various natural conditions, during and after the pile installation. Earlier, a cylindrical cavity expansion method has been employed by various researchers for simulating the pile installation process numerically, where the driving process has been replicated by expanding a pre-defined cylindrical hole horizontally (Carter et al., 1979; Randolph et al., 1979). In this regard, a finite element (FE) based numerical framework can also be adopted; however, the excessive distortion of the adjacent soil elements associated with the pile driving process makes such simulations very challenging (Dijkstra et al., 2011). In order to address this issue, a updated Lagrangian or coupled Eulerian-Lagrangian (CEL) based FE framework have often been adopted in recent times (Sheng et al., 2005; Qiu et al., 2010). In the updated Lagrangian framework, the mesh nodes are fixed and mapped with the material point, which may result in excessive distortion of the mesh with the continued deformation of the material under consideration (Hamann et al., 2014). Though the Lagrangian mesh helps in defining the soil-pile interaction and material tracking, the associated severe mesh distortion requires special attention while simulating a large deformation problem like pile driving. On the other hand, the mesh nodes are fixed with the spatial coordinates in a coupled Eulerian-Lagrangian framework and the material flow does not affect the mesh geometry, which make it suitable for pile driving problems. Although, both the methods are widely used for simulating large deformation problems, their efficacy in modeling the pile driving process is yet to be investigated.

The present study examines the effectiveness of the Lagrangian and CEL formulation for simulating the pile driving process. In this regard, a Mohr Coulomb type constitutive model has been selected to capture the stress-strain response of the soil; whereas the pile has been modeled by a linear elastic material. The finite element software, ABAQUS has been used for replicating the driving process within a three-dimensional domain. A penalty stiffness based master-slave contact has been applied to model the soil pile interface. Results obtained from three different mesh discretization have been compared to check the mesh effect in these two formulations. Further, the evolution of horizontal, axial, shear stresses and strains at a particular soil depth has been explored during the penetration process and compared for the two formulations. In addition, the stress variation along horizontal paths for a given depth of penetration and the influence of penetration rate and soil-pile interface friction have also been examined for these two different formulations. The phenomenon of friction fatigue and residual stress as observed in driven piles are further explored employing the updated Lagrangian formulation.

2 NUMERICAL SIMULATION

2.1 *Soil geometry and boundary conditions*

A 3D geometry has been selected to simulate the driving of a 10 m long and 1 m diameter pile through a uniform sand layer. The length and width of the soil domain has been kept as 15 m and it is same for both the updated Lagrangian and CEL framework. The pile has been modelled as a Lagrangian element for both the cases while, the soil has been modelled by Lagrangian and Eulerian element in the updated Lagrangian and CEL formulation, respectively. In case of updated Lagrangian approach, the depth of soil domain has been selected as 16 m; whereas, for CEL formulation an additional 2 m void space has been provided on top of the soil as depicted in Fig. 1. This additional space will take care of the flow of soil material removed by the pile during the penetration process. In order to reduce the computation time only the one-fourth part of the soil domain has been considered in this study. For this purpose, a L-shaped rigid plate has been provided at the planes of symmetry as shown in Fig. 1, which ensures the soil movement only in the one-fourth domain and acts as an axis of symmetry (Sheng et al., 2005). The initial stress has been generated through the body forces in the simulation.

Velocity boundary conditions have been employed at the base of the soil domain in order to restrain the soil movement in vertical and horizontal directions. In addition, the lateral surfaces of the soil domain have been restrained to move in the horizontal directions by applying velocity constrains. A complete fixity condition has been imposed on the rigid plate to restrain its movement in any of the directions. The rate of the pile penetration has been kept constant for both the cases by applying velocity boundary conditions of 1 m/s at the pile head.

In order to prevent unwanted rotation of the pile, zero horizontal displacement boundary conditions have been imposed on all the pile nodes.

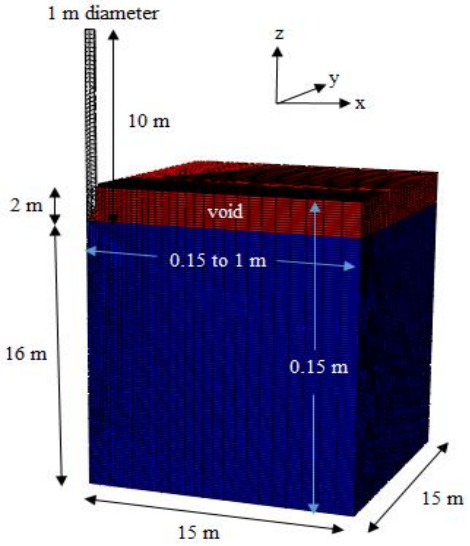

Fig. 1: Three dimensional soil-pile domain along with the mesh discretization.

2.2 *Soil parameters and contact modelling*

The Mohr Coulomb soil model has been selected to capture the stress-strain response from the simulations and for this purpose the material parameters have been adopted from Konkol (2015). The soil and pile parameters have been reported in Table 1 and 2, respectively.

The soil-pile interface has been modelled through the Coulomb friction model. The coefficient of friction has been calculated from the interface friction angle as reported in the literature and is equal to 0.21. A general contact has been applied at the interface which considers a master-slave (surface-surface) based penalty method and allows very small penetration between the master-slave surfaces. As CEL method requires explicit time integration scheme, an explicit analysis has been performed for the CEL framework.

Table 1: Soil properties used in the FE formulation

Submerged soil density (kg/m^3)	877
Young Modulus (MPa)	35.7
Poisson's ratio	0.27
Effective friction angle	35.2
Dilation angle (°)	9.0
Effective cohesion (kPa)	1.0
Coefficient of earth pressure	0.424

Table 2: Pile properties used in the FE formulation

Pile density (kg/m^3)	Young Modulus (MPa)	Poisson's ratio
2300	17000	0.12

2.3 *Mesh size*

Due to the high stiffness of the pile, very small deformation is expected for the pile, and hence, the pile has been discretized into larger size elements with 0.25 m element length. The influence of penetration would be higher near the pile and such effects will reduce with increasing radial distance from the pile. Hence, a single biased mesh has been adopted for discretization of the soil domain with smaller element sizes near to the pile. Further, in order to explore the influence of different mesh discretization on the predicted soil-pile response for both the formulations, three single biased meshes, namely coarse, fine and very fine, have been applied for the soil domain in this study. The corresponding element sizes and total element numbers for these three different meshes have been listed in Table 3. The soil elements have been discretized in such a way that an aspect ratio of 1 can be maintained near the pile. For this purpose, the depth of the element has been kept constant, i.e. equal to the length of the smallest soil element, for the complete soil domain. Hence, the depth of the elements has been kept as 0.4 m, 0.2 m and 0.15 m, respectively in the case of coarse, fine and very fine mesh. It is important to note that for the fine and very fine mesh, the size of elements near the pile is within the range of 0.5-1 times of the smallest pile element, which is often recommended to minimize the convergences issues while using updated Lagrangian formulation (Sheng et al., 2005).

Table 3: Mesh dimensions

Name	Size (m)	Elements
Coarse	0.4 to 1 m	21160
Fine	0.2 to 1 m	72000
Very fine	0.15 to 1 m	116523

3 RESULTS AND DISCUSSIONS

This section comprises a detailed discussion over the mesh convergence study, evolution of stress-strain at a given depth, shaft and toe resistances during the driving process, and comparison such responses obtained from the two different formulations, i.e. updated Lagrangian and coupled Eulerian-Lagrangian.

3.1 *Mesh convergence*

As mention earlier, three meshes named as coarse, fine and very fine mesh have been selected for the mesh convergence study. The evolution of axial reaction forces, captured in updated Lagrangian and CEL frameworks, from these three mesh have been plotted in Fig. 2. It can be observed that the coarse Lagrangian mesh exhibits large oscillation which is not present in the finer meshes. This might be due to the uneven load sharing in the coarser mesh which results in the sharp changes in axial reaction force when the pile corner passes through a soil node. Similar response is also observed for the coarse mesh of CEL; however, the oscillations in CEL are much higher than the updated Lagrangian approach. Although the results obtained from CEL and updated Lagrangian are quite comparable when considered for a particular mesh type, one should note that in case of updated Lagrangian the results from fine and very fine mesh attain almost same values (Fig. 2) in comparison to CEL, where the mesh convergence is yet to get achieved. To investigate further, the evolution of von Mises and mean stresses for a point located at a depth of 5 m and 0.8D radial distance away from the pile surface have been plotted in Fig. 3 for these three meshes. It can be noticed that the stresses obtained from the coarse mesh are markedly different for these two formulations, while the stresses from the fine and very fine mesh are still within a comparable range. Hence, it can be inferred that the mesh convergence can be achieved much faster

for the updated Lagrangian framwork. In this study, the results of very fine single biased mesh have been selected for further analysis.

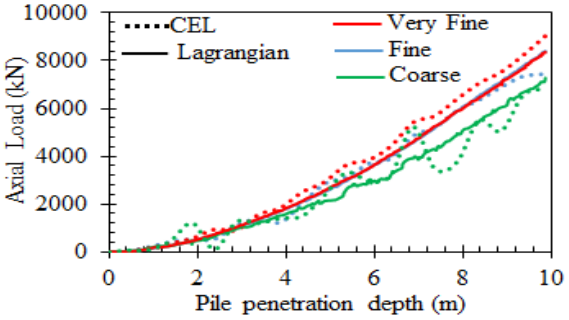

Fig. 2: Evolution of axial load with penetration depth of the driven pile as obtained from CEL and Lagrangian formulations for very fine, fine and coarse mesh.

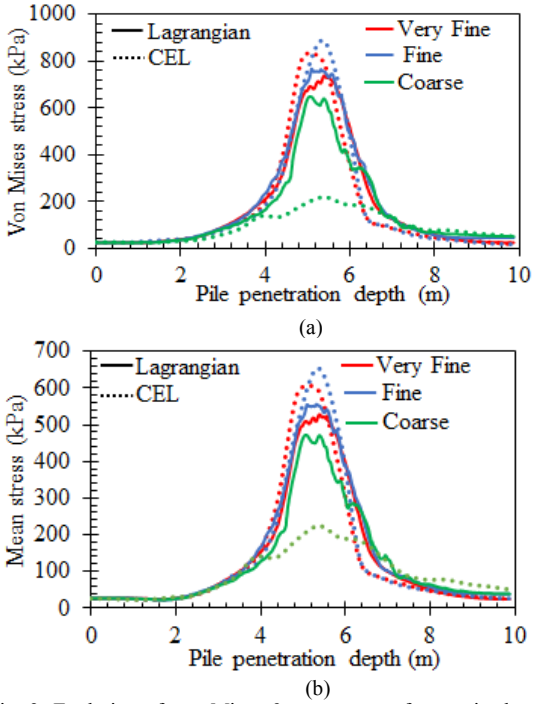

Fig. 3: Evolution of von Mises & mean stress for a point located at a depth of 5 m and 0.8D radial distance away from the pile surface as obtained from CEL and Lagrangian formulations for very fine, fine and coarse mesh.

3.2 *Comparison of stress-strain response*

In this section, the evolution of stress and strain responses at a point located near the pile-soil interface during the complete penetration process have been compared for the CEL and updated Lagrangian approaches. For this purpose, the horizontal, shear and axial components of stresses and strains obtained at 5 m soil depth has been reported in this paper. It is important to note that in case of CEL approach, the penetration process is simulated by replacing the Eulerian soil material by the Largangian pile element. The deformation of the soil can be tracked down by the Eulerian volume fraction (EVF), which computes the volume of Eulerian mesh filled with the soil material. The Eulerian mesh is completely filled with the soil prior to the penetration and attains an EVF value of 1 expect at the additional 2 m void space on the top, where zero EVF value has been assigned (Fig. 1). An EVF value of 0 indicates the absence of soil in the Eulerian mesh and referred as void space. During the pile penetration process, the Eulerian soil material present in the vicinity of the progressing pile gets replaced by the Lagrangian pile element resulting in reduction of the EVF value. The EVF value finally reduces to zero for a zone extending up to a radial distance of 0.5D m form the axis of penetration. Since, the stress and strain are computed as a volume fraction weighted average of the material present inside the Eulerian mesh, the stress and strain components reduce to zero in this null EVF zone after the penetration. In order to compare the stress-strain evolution up to the complete penetration depth, the stress-strain responses have been reported at 0.8D m radial distance from the axis of penetration, so that results can be obtained even from the coarser mesh.

During the pile penetration process, a soil zone just beneath the pile tip experiences excessive axial compression. In addition, the soil tends to expand radially to bear such extreme compression. As this soil zone passes through the pile cone and reaches over the pile shaft, the soil gets relaxed (loosen) and the axial compression changes into axial expansion. Further, the radial expansion ceases and the horizontal earth pressure tries to compress the soil radially against the pile shaft. This behavior can be observed from the plastic strain plots obtained at 5 m soil depth and depicted in Fig. 4(a). The negative and positive sign indicate the compression and expansion, respectively. As the pile tip crosses the 5 m depth, the nature of axial strain (ε_{zz}) changes from compression to expansion. Similarly, the horizontal strain (ε_{xx}) becomes compressive after the penetration at 5 m depth. The development of plastic strain is minimal till the penetration depth reaches the observation point, i.e. 5 m (Fig. 4a), and then after a drastic change can be noticed in the strain profile. The soil relaxation might have attributed to such sudden change which continues until the plastic strain gets fully mobilized and finally leading to a constant magnitude (Fig. 4a). Though similar trend can be noticed from the CEL and updated Lagrangian strain plots, a significant difference can be observed in their magnitude, especially in post penetration regime. The reason could be the different strain measures used by the finite element software, ABAQUS for the CEL and Lagrangian formulations.

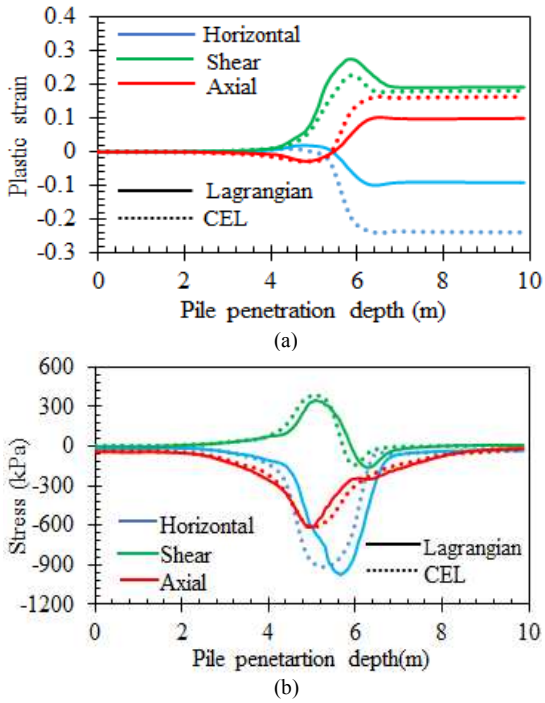

Fig. 4: Comparison between (a) plastic strain and (b) stress responses obtained from the updated Lagrangian and CEL formulations for the point located at a 5 m depth and 0.8D radial distance away from the pile surface.

Figure 4(b) shows the evolution of horizontal (σ_{xx}), shear (σ_{xz}) and vertical (σ_{zz}) stresses at 5 m soil depth from the updated Lagrangian and CEL approaches. It can be observed that, the stress magnitudes first increase with the penetration but a sudden stress drop can be noticed as the pile passes through the observation point, i.e. 5 m depth. This kind of behavior has been also reported in Lehane (1992), Robinsky and Morrison (1964) and might be due to the loosening of sand, which has been explained in previous section. Comparison between the updated Lagrangian and CEL results shows that axial and shear stress obtained from the CEL method are slightly higher than the updated Lagrangian. Figure 5 shows the deformed contour for both the simulations and the deformation pattern obtained from the updated Lagrangian framework is consistent with the pattern reported in Robinsky and Morrison (1964). The stresses captured from both the methods are comparable with each other.

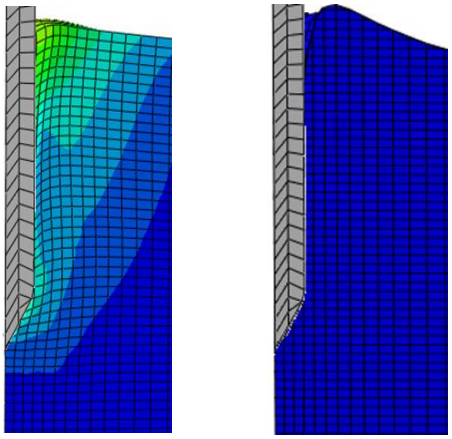

(a) (b)

Fig. 5: Deformed mesh configuration after 5 m penetration in (a) Lagrangian and (b) CEL formulation.

3.3 *Stress along the horizontal path*

In this section, the stresses obtained from the updated Lagrangian and CEL methods have been compared along the different horizontal paths to examine their efficacy in capturing stress evolution in the radial direction. For this purpose, two horizontal paths passing through 7.5 m and 10 m depths have been selected. Figure 6 shows the comparison of horizontal stresses along these two paths, when the pile has reached at 5 m penetration depth. Slight variation has been observed in the CEL and updated Lagrangian stresses near the soil-pile interface. This variation reduces with increasing horizontal distance from the interface and practically no difference has been recorded after a radial distance of magnitude 7D.

3.4 *Toe and shaft resistance*

The toe and shaft resistance obtained from the updated Lagrangian and CEL formulations have been compared in this section. The effect of interfacial friction has also been examined in this study by employing two different coefficient of friction (COF) values, i.e. 0.1 and 0.2. The comparison of toe and shaft resistance has been depicted in Fig. 7(a) and (b), respectively. It can be observed that the toe and shaft resistance obtained from the very fine and fine updated Lagrangian mesh are almost similar. On the contrary, fine and very fine CEL mesh results have significant variations with a difference of nearly 25 % in toe and 15 % in shaft resistance after the 10 m penetration. It can be observed that for both the frameworks toe resistance has much higher contribution than the shaft resistance. Further, it has been noticed that the interfacial friction has significant impact on both the toe and shaft resistance (Fig. 7a&b). On reducing the interfacial friction to half of its initial value, the toe resistance reduces by 27%, while the shaft resistance shows major reduction of 60% from the original value.

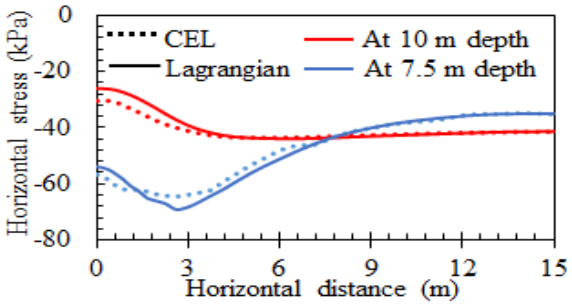

Fig. 6: Horizontal stress variation along two horizontal paths in Lagrangian and CEL formulation.

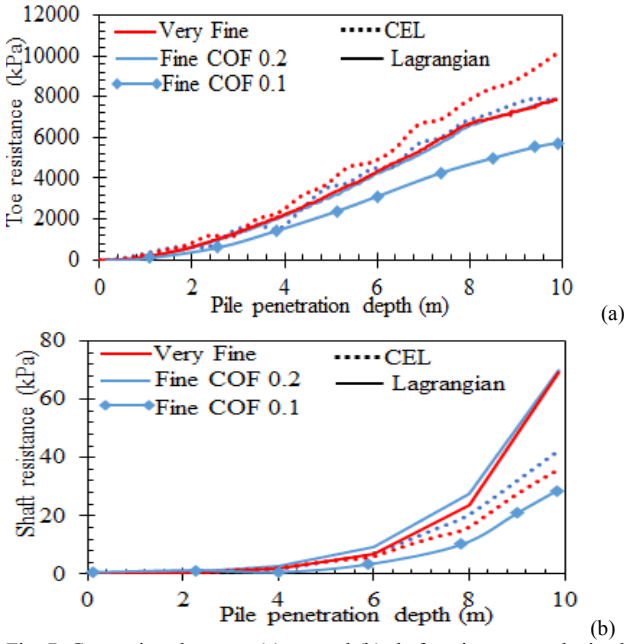

Fig. 7: Comparison between (a) toe and (b) shaft resistance as obtained from very fine and fine mesh CEL and Lagrangian formulations.

3.5 *Rapid penetration*

This section comprises a detailed discussion on the effect of penetration rate on predictions from updated Lagrangian and CEL frameworks. For this purpose, the results obtained with two different penetration velocities have been compared. The first case has named as static case with a penetration rate of 0.25 m/s and the second one is termed as rapid case, where the penetration rate has been increased four times, 1 m/s. Although, the employed Mohr-coulomb model is rate independent, inertia may still affect the pile penetration simulation results. Hence, this exercise could provide us a general idea about the effects of penetration rate on these two frameworks. The evolution of axial load with pile penetration depth as obtained from the updated Lagrangian and CEL methods for very fine and fine mesh have been plotted in Fig. 8 (a) and (b), respectively. It is interesting to note that for the updated Lagrangian method, load-displacement response does not get affected by the penetration rate and all the curves attain almost similar path (Fig 8a); whereas, the CEL result has significant effect of penetration rate as shown in Fig. 8(b) and the rapid case has reported higher axial load then the static case. The comparison of various system energies reveals that the contribution of kinetic energy is very less compare to the total internal energy,

which eliminates the possibility of inertial effects behind such variation. Another possible reason could be the explicit nature of the CEL solver employed in this study. The stable time increment requires in the explicit analysis depend upon the mesh refining and total time assigned for the event (ABAQUS Analysis User's Manual, 2014) and hence, the penetration rates might have an impact on the simulation results.

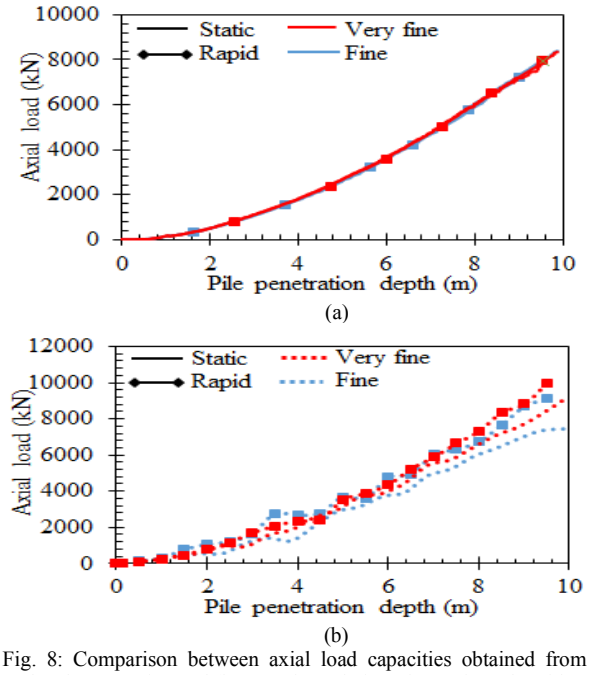

Fig. 8: Comparison between axial load capacities obtained from (a) updated Lagrangian and (b) CEL formulations for static and rapid case.

3.6 *Friction fatigue analysis*

Skin friction at a particular soil horizon can vary as the pile penetrates deeper into the soil and this phenomena is known as friction fatigue (White and Lehane, 2004). An attempt has been made in this paper to investigate the friction fatigue process through the numerical simulation. In this regard, four different elements have been selected on the soil-pile interface, located at the height (h) of 3D, 4D, 5D and 7D from the pile tip, where D is the diameter of the pile. The shear stress (σ_{xz}) and shear force responses obtained at these elements have been plotted against the depth from the ground surface and depicted in Fig. 9. Only the results obtained from the updated Largangian analysis with COF value of 0.2 have been reported for this purpose. The distribution of the shear stress (σ_{xz}) component for the selected elements has been plotted in Fig. 9(a); whereas the contact shear force obtained for the selected elements at the pile-soil interface has been presented in Fig. 9(b).It can be observed that at a soil horizon, nearly same shear stress and force have been obtained from all the elements, expect the elements located nearer to the pile tip. This behavior can be explained through the shear stress evolution plotted in Fig. 4. As discussed earlier, when soil elements pass through the sharp corner of the pile cone a sudden decrease in the shear stress has been noticed, which is followed by a nearly uniform shear stress profile (Fig. 4). As a result, maximum shear stress mobilization at any soil horizon occurs when the pile tip is located nearest to it. This could be a reason for the drastic variation in the shear stress and forces obtained from the elements located at a height of 1D from the pile tip. From the above discussion it can be conclude that the friction fatigue phenomena could be possible even from the monotonic loading case; however, its extent is limited only in a narrow region nearer to the pile tip.

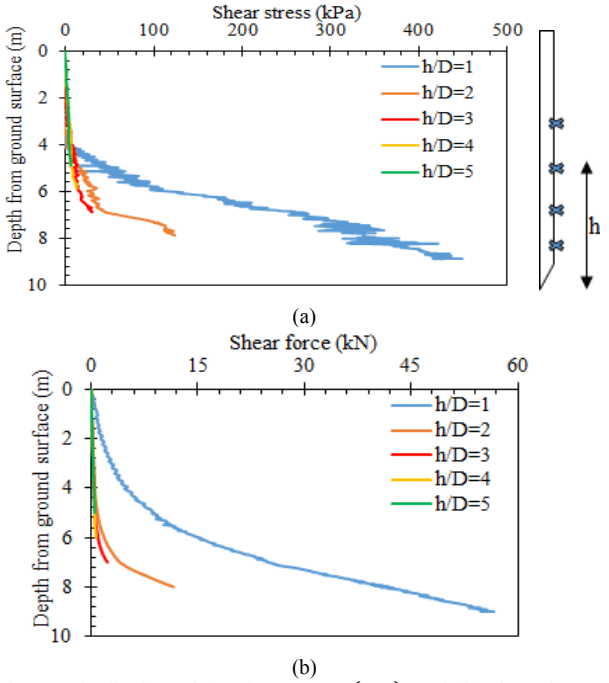

Fig. 9: Distribution of (a) shear stress (σ_{xz}) and (b) shear force at various depths from the ground surface as obtained at pile-soil interface.

3.7 *Residual Stress analysis*

The stress induced in the soil during the penetration process usually gets ignored prior to the pile load test; however, this could be a concern if contribution of such residual stress turns out to be significant, especially on the distribution of mobilized shaft friction and end bearing. The piles installed in the sand can develop residual load more than 0.4 times of their ultimate uplift capacity (Alawneh and Malkawi, 2000). In order to find the nature and magnitude of the residual load, a simulation has been carried out with the updated Lagrangian framework. For this purpose, after the end of the driving process, the loading i.e. velocity boundary condition has been deactivated, and the axial shear force and stress distribution on the pile surface has been recorded. A ramp type unloading process has been employed instead of an instantaneous one. The shear force and stress (σ_{xz}) distribution just at the end of driving process and after releasing the load has been depicted in the Fig. 10 along with an intermittent distribution recorded during the unloading process. It can be noticed that the shear force, which acts on the pile surface in upward direction during the driving process, completely reverses its direction after removal of the driving load. Residual load induced such complete mobilization of upward shear stress along the pile surface can also be noticed in the experimental studies reported by Fellenius (2002). The intermittent distribution shows the transition of the shaft shear force during the unloading process (Fig. 10). The maximum residual shear force has been noticed towards the pile tip which is nearly 50% of the shaft resistance (530 kN) noticed in the driving phase. Though the shaft resistance has minimal contribution in the total load carrying capacity, the 270 kN residual load could be a reason for the over estimation of shaft resistance during the pile load test. The shear stress distribution plot presented in Fig. 10(b) also conforms to the obtained force distribution.

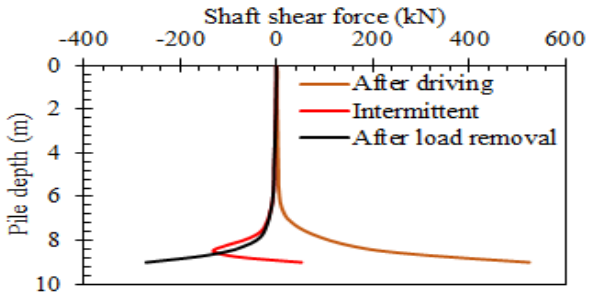

(a)

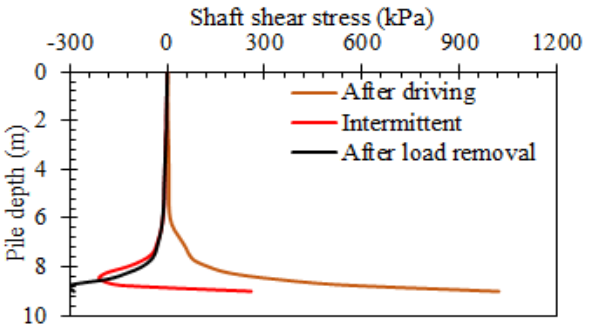

(b)

Fig. 10: Distribution of shaft (a) shear force and (b) shear stress (σ_{xz}) along the pile length just after driving, post-driving complete load removal and intermittent post-driving unloading stage.

4 CONCLUSIONS

This paper present a comparative study to examine the efficacy of updated Lagrangian and CEL frameworks in simulating pile driving process involving large deformation. In this regard, a 3D soil domain has been selected, which has further been discretized by employing three different single biased meshes. The stress-strain response, toe and shaft resistance as obtained from the two formulations have been compared for all these three types of meshes. The effect of penetration rate on the simulation results from the two formulation has also examined to get better understanding of pile driving rate. In addition, the friction fatigue and residual load distribution over the pile shaft have been simulated from the updated Lagrangian approach. Following are the salient observations from the present study:

- The mesh convergence of updated Lagrangian framework has been noticed to achieve even with the medium fine mesh; whereas, CEL performance depends highly on the mesh discretization and requires extremely fine mesh to achieve the converged simulation. As CEL approach works only with the explicit time integration scheme, it takes less solution time than the updated Lagrangian approach, which works precisely with implicit scheme in Abaqus Standard.
- During the driving process, a sudden stress drop has been noticed in both the formulations once the pile tip moves away from the observation point, which indicates the loosening of sand adjacent to the pile shaft. Noticeable variations are obtained in the magnitude of various plastic strain components for the two formulations, which might have attributed by the different strain measures used in these formulations.
- The horizontal stresses obtained from these two frameworks have shown slight variation near the interface; however, these variations diminish beyond 7D radial distance from the soil-pile interface and converge to similar value towards the domain boundary.
- The toe and shaft resistance estimated from the updated Lagrangian approach are nearly similar for the different meshes; whereas, a significant difference has been noticed in the resistance magnitudes while considering various mesh sizes following CEL approach. The interface friction coefficient has a major impact on the shaft resistance compared to the toe resistance.
- The penetration rate does not influence the updated Lagrangian framework; however, the CEL results exhibit significant impact of the driving velocity. At the end of penetration process, nearly 18 % increase in the axial load has been noticed for the rapid case compared to the static one, which might be a numerical artifact due to the explicit solver used in the CEL approach.
- The friction fatigue phenomenon can be observed in the pile derived through monotonic loading however, its extent is limited in a narrow region near the pile tip.
- The shear force induced along the pile shaft completely reverses its direction after the removal of the loading and its magnitude is nearly 50% of the initial shaft resistance.
- Overall the performance of updated Lagrangian method has been observed to be better than the CEL approach in terms of mesh convergence and accuracy; however, it takes more computation time and difficult to apply with extremely fine mesh. On the contrary, CEL provides efficient results incurring lesser computation time.

5 ACKNOWLEDGEMENTS

The authors would like to thank SERB (Grant No. ECR/2018/002141) for the financial support toward carrying out part of this research.

6 REFERENCES

ABAQUS Analysis User's Manual (2014). Version 6.14, Dassault Systèmes Simulia, Inc.

Alawneh A.S. and Malkawi A.I.H. (2000). "Estimation of post-driving residual stresses along driven piles in sand." Geotechnical Testing Journal, Vol. 23, No. 3, pp. 313-326.

Carter J.P., Randolph M.F. and Wroth C.P. (1979). "Stress and pore pressure changes in clay during and after the expansion of a cylindrical cavity." International Journal for Numerical and Analytical Methods in Geomechanics, Vol. 3, No. 4, pp. 305-322.

Dijkstra J., Broere W. and Heeres M.O. (2011). "Numerical simulation of pile installation." Computers and Geotechnics, Vol. 38, pp. 612-622.

Fellenius B.H. (2002). "Determining the true distributions of load in instrumented piles." International Deep Foundation Congress, Orlando, Florida. Vol. 2, pp. 1455-1470.

Hamann T., Qiu G. and Grabe J. (2014). "Application of a coupled Eulerian-Lagrangian approach on pile installation problems under partially drained conditions." Computers and Geotechnics, Vol. 63, pp. 279-290.

Konkol J. (2015). "Numerical estimation of the pile toe and shaft unit resistances during the installation process in sands." Studia Geotechnica et Mechanica, Vol. 37, No. 1, pp. 37-44.

Lehane B. (1992). "Experimental investigations of pile behaviour using instrumented field piles." Doctoral Dissertation, Imperial college of Science, Technology and Medicine, University of London.

Qiu G., Henke S. and Grabe J. (2010). "Application of a coupled Eulerian-Lagrangian approach on geomechanical problem involving large deformations." Computers and Geotechnics, Vol. 38, pp. 30-39.

Robinsky E.I. and Morrison C.F. (1964). "Sand displacement and compaction around model friction piles." Canadian Geotechnical Journal, Vol. 1, No. 2, pp. 81-93.

Randolph M.F., Carter J.P. and Wroth C.P. (1979). "Driven piles in clay-the effects of installation and subsequent consolidation." Geotechnique, Vol. 29, No. 4, pp. 361-393.

Sheng D., Eigenbrod K.D. and Wriggers P. (2005). "Finite element analysis of pile installation using large-slip frictional contact." Computers and Geotechnics, Vol. 32, pp. 17-26.

White D.J. and Lehane B.M. (2004). "Friction fatigue on displacement piles in sand." Geotechnique, Vol. 54, No. 10, pp. 645-658.